

## **General Disclaimer**

### **One or more of the Following Statements may affect this Document**

- This document has been reproduced from the best copy furnished by the organizational source. It is being released in the interest of making available as much information as possible.
- This document may contain data, which exceeds the sheet parameters. It was furnished in this condition by the organizational source and is the best copy available.
- This document may contain tone-on-tone or color graphs, charts and/or pictures, which have been reproduced in black and white.
- This document is paginated as submitted by the original source.
- Portions of this document are not fully legible due to the historical nature of some of the material. However, it is the best reproduction available from the original submission.

# Heaterless Ignition of Inert Gas Ion Thruster Hollow Cathodes

(NASA-TM-87086) HEATERLESS IGNITION OF  
INERT GAS ION THRUSTER HOLLOW CATHODES

N85-34177

(NASA) 23 p HC A02/MF A01

CSSL 21C

Unclas

63/20 22223

Michael F. Schatz  
*Lewis Research Center*  
*Cleveland, Ohio*

Prepared for the  
18th International Electric Propulsion Conference  
cosponsored by the AIAA, JSASS, and DGLR  
Alexandria, Virginia, September 30–October 2, 1985

**NASA**



# HEATERLESS IGNITION OF INERT GAS ION THRUSTER HOLLOW CATHODES

Michael F. Schatz  
National Aeronautics and Space Administration  
Lewis Research Center  
Cleveland, Ohio 44135

## Abstract

Heaterless inert gas ion thruster hollow cathodes were investigated with the aim of reducing ion thruster complexity and increasing ion thruster reliability. In this study, cathodes heated by glow discharges were evaluated for power requirements, flowrate requirements, and life limiting mechanisms. In addition, an accelerated cyclic life test was completed.

## Nomenclature

$J_A$	anode current
$J_C$	cathode current
$J_{GD}$	glow discharge current
$J_I$	insert emission current
$J_{IGSC}$	ignitor supply short circuit current
$J_K$	keeper current
$J_{KL}$	keeper supply current limit
$\dot{m}$	mass flowrate
SCC	standard cubic centimeters (volume)
SCCM	standard cubic centimeters per minute (flowrate)
	} standard conditions - 21 °C and 760 mm Hg
$V_A$	anode voltage
$V_B$	breakdown voltage
$V_C$	cathode voltage
$V_{GD}$	glow discharge voltage
$V_{IGOC}$	ignitor supply open circuit voltage
$V_K$	keeper voltage
$V_{KOC}$	keeper supply open circuit voltage

## Introduction

In recent years, electrostatic ion thruster research has been heavily focussed on operation with inert gas propellants because advantages of inert gases over mercury, the propellant previously used, were recognized.<sup>1,2</sup> In addition, the NASA Lewis Research Center, Hughes Research Labs and others have studied ways to simplify ion thruster systems.<sup>3,4</sup> Not surprisingly, these two trends overlap; use of the inert gases suggests natural simplifications to ion thruster systems (e.g., replacement of vaporizers, necessary for Mercury propellant systems, with a simpler glow control scheme on inert gas systems<sup>3</sup> and potential

reductions in power processor requirements). Continuing in this spirit, the NASA Lewis Research Center has pursued work on heaterless inert gas ion thruster hollow cathodes.

## Description of Hollow Cathode Operation

### Standard Hollow Cathode Ignition

Ignition of the standard hollow cathode begins with the activation of the heater power supply, which heats the cathode to approximately 1000 °C,<sup>5</sup> followed by the introduction of propellant into the cathode as shown in Fig. 1. The keeper and ignitor supplies are then activated, the gas breaks down electrically and an arc discharge ignites. Stable hollow cathode arcs require a copious source of electrons which the insert provides by the mechanism of field enhanced thermionic emission.<sup>6,7</sup> In this scenario, the insert must be heated to a temperature of approximately 1000 °C over a region large enough such that, in combination with the electric field generated by a nearby, dense plasma, the insert emits enough electrons to maintain a stable arc.

With mercury as a propellant, the hollow cathode heater serves two purposes during ignition. First the heater prevents mercury from condensing inside the cathode before ignition. Second, the heater raises the temperature of the cathode to a level at which significant thermionic electron emission may occur from low work function surfaces. After ignition of the arc, the cathode heats through ion bombardment; thus, the heater is no longer needed and is usually turned off.

When an inert gas replaces mercury, the cathode heater is not needed to prevent condensation. Further, hollow cathodes in laboratory inert gas ion thrusters have been started without a hollow cathode heater by flooding the cathode during ignition.<sup>11</sup> In addition, although it has been demonstrated that reliable heaters can be constructed, hollow cathode heaters are viewed by some as a failure prone component and have been shown to be sensitive to fabrication procedures.<sup>5,8,9</sup> Finally, hollow cathode heaters require either a dedicated power supply for each heater or a switching scheme for sharing a common supply. Both scenarios entail increased mass and intricacy for the overall system. Ultimately, heaterless ignition of ion thruster hollow cathodes should contribute to more reliable ion thruster designs with a lower parts count.

### Heaterless Cathode Ignition

Before the hollow cathode can ignite without a heater, the propellant must breakdown electrically without a heater. (Note that "ignition" means establishing a low voltage (10 to 40 V) high current (>1 A) electrical discharge (i.e., an "arc"), while "breakdown" implies the onset of an electrical discharge in some mode (not necessarily an arc). Thus, it is important to first understand

what mechanisms govern the heaterless breakdown of propellant. In our investigation, Paschen's law served as the model of electrical breakdown. Paschen's law states that when breakdown voltage (VB) is plotted as a function of P times D (P\*D), where P is the gas pressure between two electrodes and D is the distance between the electrodes, the breakdown voltage minimizes for a unique value of P\*D (called the Paschen minimum). Paschen's law has been experimentally established for well defined P (static gases) and D (parallel plate geometry) (Fig. 2);<sup>10-12</sup> however, neither criteria is satisfied in the standard hollow cathode geometry because the geometry is nonplanar and the pressures are nonstatic in the breakdown region between the cathode orifice plate and the keeper. Nevertheless, one would expect the trends to remain the same, i.e., when breakdown voltage is plotted as a function of P\*D for the hollow cathode, perhaps a Paschen minimum could be found near the 1 MMHG\*CM value characteristic of well defined P\*D cases (Fig. 2). Examining the standard hollow cathode under this assumption, with reasonable estimates of P and D, the P\*D product is seen to be well below this characteristic value ( $P*D = (0.001 \text{ MMHG}) * (0.15 \text{ cm}) = 0.00015 \text{ MMHG*CM}$ ). The Paschen theory would qualitatively explain the experimental observation that the heaterless ignition of standard hollow cathodes requires high flow rates - increasing the P\*D product by increasing P through increased flowrate brings the breakdown voltage down to the level satisfied by the open circuit voltage of the ignitor supply. Demanding heaterless ignition at reasonable ignitor supply voltages (<1 kV) implies that electrical breakdown in heaterless hollow cathodes should occur near Paschen minimum breakdown voltages, typically on the order of 200 to 400 V for most gases (Fig. 2).

Under Paschen's law, the breakdown voltage for the heaterless hollow cathode can be lowered in a number of ways (e.g., lengthening D, increasing P, "seeding" the propellant with a low ionization potential material,<sup>12</sup> etc.). In this study, the goal was to modify the standard hollow cathode by disturbing the geometry as little as possible while achieving heaterless breakdown and ignition at normal operating flow rates, thereby preserving the proven lifetime of the standard ion thruster hollow cathode and insert.<sup>13</sup>

#### Heaterless Cathode Geometries

##### Original Heaterless Cathode Design

To our knowledge, Aston first attempted to construct a heaterless ion thruster hollow cathode.<sup>14</sup> Instead of an oxide impregnated insert, Aston placed a tantalum emitter tube inside the cathode, which, unlike the insert in the standard ion thruster hollow cathode (Fig. 1), is electrically isolated from the cathode body. Aston achieved breakdown and ignition but at the expense of crystallization and melting of the emitter tube.<sup>14</sup> In our experiments, Aston's idea was modified by isolating a porous tungsten insert from the cathode body (Fig. 3). In so doing, the breakdown region is moved to the interior of the cathode, increasing the P\*D product by raising P from approximately 0.001 MMHG to 1 MMHG while keeping D roughly constant. Heaterless configurations, were tested in diode arrangements (within a bell jar), and one configuration was operated as

a main cathode in the discharge chamber of a 30 cm J series ion thruster.

Figure 4 depicts the power supply arrangement and gas flow schematic for the heaterless cathode (compare with the power supply arrangement in standard hollow cathode (Fig. 1)). In addition to the keeper and anode supplies shown for the standard hollow cathode, the heaterless cathode experiments included a cathode supply and an ignitor supply. In practice, the cathode supply was little used and later eliminated. Note that in most laboratory configurations, the keeper supply for the standard hollow cathode consists of two separate supplies - a low voltage high current supply and a high voltage low current supply. Switching from the standard to the heaterless hollow cathode eliminates the heater power supply (compare Figs. 1 and 4). After arc ignition the cathode and the insert were linked electrically by manually closing a knife switch or vacuum relay. In the initial experiments, an absolute pressure gauge tapped in upstream (in the direction opposite of propellant flow) of the cathode orifice estimated the static pressure inside the hollow cathode to within an order of magnitude.

##### Modified Heaterless Cathode Design

The original heaterless hollow cathode design was altered as our understanding of heaterless ignition increased. First, to better protect the sintered porous tungsten matrix of the insert during ignition, a tantalum tube with a thoriated tungsten plate (an "insert cover") was placed over the insert (Fig. 5). Except for the orifice sizes (dimensions G and H), this geometry is identical in appearance to existing hollow cathode enclosed keeper designs, in which the insert cover and cathode body (with their orifice plates) in this experiment are otherwise known as the cathode and enclosed keeper, respectively. In the enclosed keeper cathode G is less than H, whereas in the heaterless covered insert cathode G is greater than H, thus changing the site of flow restriction and enabling the covered insert design to ignite heaterlessly at reasonably low values of ignition voltage. The reader should compare Fig. 3 to Fig. 5 to contrast physical and nominal differences between the original and modified heaterless cathode designs.

Next, during ignition the cathode was flooded with a measured amount of propellant. Lab experience with heaterless ignition of standard hollow cathodes and the success of Hughes Research Labs with rapid heaterless ignition of hollow cathodes using this technique inspired the change.<sup>15</sup> To begin a pulsed flow start, a fixed volume of propellant (approx. 12 to 50 SCC) accumulates between the manual leak valve and the solenoid valve (see Fig. 4). With the keeper and ignitor supplies on at open circuit voltages, the solenoid valve opens and the accumulated gas floods the cathode-insert region. Then the gas breaks down electrically and the cathode ignites. The manual leak valve establishes the normal operating pressures inside the cathode after ignition because it meters gas flow at a preset low flow condition. After the arc extinguishes and the solenoid valve closes, the manual leak valve continues to meter gas into the accumulator region between the leak valve and the solenoid valve until the static pressures on both sides of the manual leak valve equalize. (This

process took about 10 min in our experimental configuration.) It is important to note that the additional amount of propellant required to ignite cathodes in this manner should not significantly add to the mass of an actual flight system, even if the system is to operate for thousands of ignition cycles. For example, assuming 50 SCC of xenon gas per pulsed flow, 1000 ignition cycles of a single cathode would require approximately 260 g of propellant.

Finally, the knife switch, used to electrically connect the insert to the cathode after arc ignition, was replaced with a high voltage, high current diode (Fig. 4). During the breakdown of the propellant, the diode is reversed biased, effectively isolating the cathode and the insert. After arc ignition, the diode is forward biased and the emission current divides itself between the cathode and the insert as the operating conditions warrant.

### Experimental Results

#### Results of Original Heaterless Cathode Test

Breakdown voltage as a function of flowrate was recorded for the standard hollow cathode (without a heater) and for the heaterless hollow cathode configurations (Figs. 6 to 9). Because increases in flowrate cause increases in internal pressure, the plots of breakdown voltage as a function of flowrate were expected to emulate plots of breakdown voltage as a function of  $P \cdot D$ ; comparing Fig. 2 to Figs. 6 to 9 substantiates this assumption. When taking this data, the flowrate was set to a predetermined value, and the ignitor supply was ramped up until the ignitor voltage abruptly collapsed and the ignitor current suddenly increased, indicating voltage breakdown. The measured breakdown voltage for a fixed flowrate and geometry varied  $\pm 20$  percent for flowrates less than 4 SCCM and  $\pm 5$  percent for flowrates greater than 4 SCCM. Turning off the keeper, anode or cathode supplies did not affect the breakdown voltage; usually these supplies were off during the taking of breakdown voltage versus flowrate data. The breakdown voltage increased 10 percent when repeated breakdowns were measured in rapid succession; these variations were not removed from the data.

Figure 6 shows breakdown voltage (VB) as a function of flowrate for the standard 30 cm hollow cathode and insert. Note that the standard hollow cathode typically operates at approximately 5 SCCM flowrate; thus, an increase of several times the normal operating flow is required to achieve breakdown at the 1200 V open circuit voltage of the lab ignitor supplies. Data for the heaterless configurations demonstrate a much lower breakdown voltage for a given flowrate (Figs. 7 to 9). Figure 7 compares the effect of changing the cathode orifice diameter (dimension F, Fig. 3) on the breakdown voltage. Increasing the cathode orifice diameter decreases the pressure in the breakdown region; thus, at a fixed flow rate, the  $P \cdot D$  product shrinks and the corresponding breakdown voltage grows as the cathode orifice area expands. At higher flow rates, the differences disappear. Figure 8 demonstrates the effect of cathode-insert distance on breakdown voltage (dimension G in Fig. 3). The breakdown voltages are roughly equal for more than an order of magnitude change in

dimension G except at the lower flows, where uncertainties in the data may yield spurious differences. Figure 9 (configurations 2(b) and 3(a)) illustrates the breakdown voltage versus flowrate for larger geometries with two different sizes of insert and cathode body. The data is similar to that of previous geometries with the same cathode orifice diameter (compare with Fig. 8).

In general, achieving a voltage breakdown does not guarantee ignition of the hollow cathode (recall the distinction between "breakdown" and "ignition"). Figure 10, which depicts a typical power supply loadline imposed upon a typical voltage versus current characteristic for a gaseous electrical discharge,<sup>10</sup> illustrates several possible regimes of operation which depend upon the physical parameters of the discharge and upon the physical parameters of the power source. The criterion for the stability of a gaseous discharge driven by a power source is  $(DE/DI - R) > 0$ , where  $DE/DI$  is the gaseous discharge's impedance and  $R$  is the power supply's impedance at the intersection points of the loadline and the characteristic (see Fig. 10, B and D are stable points of operation while C is an unstable point of operation<sup>10</sup>). After voltage breakdown, the cathode would settle into a glow discharge, a high voltage ( $> 100$  V) low current ( $< 1$  A) mode, which would last anywhere from milliseconds to minutes. The cathode would then transition into another glow discharge or, far more typically, would transition into an arc. This behavior can be understood by recalling that the normal operating temperature of the hollow cathode is 1000 °C; the hollow cathode must reach this temperature during ignition. Instead of using a heater, a glow discharge raises the temperature of the heaterless hollow cathode. Normally, the glow discharge would couple from the insert to the keeper after breakdown because the keeper, which is at a higher potential than the cathode body, extracted the glow discharge out of the cathode body. Without the keeper, the anode could also extract the glow discharge. The glow discharge remained coupled to the keeper (or anode) during and after the transition to the arc. Raising the open circuit voltage on the keeper shortened the time spent in the glow discharge. Even before connecting the insert to the cathode body with the knife switch, the cathode voltage would measure nearly zero when the cathode was in the arc mode. The electrical discharge could not be extracted out to the keeper or anode if the keeper and anode supplies were not turned on until after the glow discharge was established or if the cathode supply was used during ignition. Without a discharge, internal cathode pressures in the 1 to 10 torr range were measured (in agreement with Ref. 14) and were observed to increase by a factor of five during arc mode operation. An optical pyrometer measured temperatures of 1000 to 1200 °C on the weld between the cathode orifice plate and the cathode body during stable arc operation.

By isolating the insert in the heaterless cathode, the ratio of insert emission current to total cathode emission current was measured and compared to results of a similar study.<sup>6</sup> In that study, insert emission current accounted for 80 to 90 of the total emission current for total emission currents up to approximately 8 A. Our observations confirmed this result; however, at around the 10 A level, the cathode orifice plate/cathode body (Fig. 11, configuration 1(b)) began to dominate

electron emission for some unknown reason. Perhaps at the higher power levels, the temperatures and/or the plasma conditions cause the cathode orifice plate/cathode body to become a thermionic emitter, or volume ionization begins to dominate electron production (i.e. the greater cathode emission is actually increased ion collection to the cathode body).

After approximately 100 breakdowns (with roughly 10 hr of arc operation accumulated over the course of testing), the inserts suffered damage on the downstream ends (Figs. 12 and 13), probably resulting from overheating and/or ion sputtering during the glow discharge. Damage to the inserts designed for the 8 cm thruster (used in configuration one) was expected since these inserts were operated in this experiment at total emission currents up to 15 A; the design operating range is in the 1 A regime.<sup>16</sup> Use of the inserts designed for the 30 cm thruster reduced but did not eliminate the erosion problem (Fig. 13 and configurations 2 and 3). The insert insulator was observed to accumulate a metallic coating, lowering the impedance between the cathode and the insert. To reduce the observed erosion, the insert cover and pulse flow starting were instituted (see results of modified heaterless cathode test).

The heaterless cathode was operated in the discharge chamber of a J series 30 cm xenon ion thruster. The main discharge was stable and a 2 A beam was extracted at reasonable thruster operating conditions. Heaterless starting was achieved without use of the keeper electrode by coupling directly to the anode. Evidence of arc damage within the discharge chamber on cathode potential surfaces was noted and later investigated. (See the following section.)

#### Results of Modified Heaterless Cathode Test

Modifications to the original heaterless cathode did not significantly affect the breakdown voltage-flowrate characteristic curve (Fig. 9) (note that the pulse flow technique was not used to take this data). The glow discharge regime was explored by plotting the time spent in glow discharge as a function of glow discharge power (Fig. 14), of flowrate (Fig. 15), and of elapsed time between successive starting attempts (i.e., spacing repetitive ignition cycles with a fixed time interval) (Fig. 16). It is thought that lessening the time spent in glow discharge would reduce erosion due to ion sputtering and/or overheating; thus, it was important to map the trends which lead to shorter glow discharge times. The ignitor supply loadline was characterized by giving the open circuit voltage and short circuit current and the input power to the cathode during the glow discharge mode by recording the glow discharge voltage and current. When taking data, the run parameters were fixed, a steady flow of propellant through the cathode was established, the ignitor supply was activated (which caused the voltage breakdown), the lifetime of the ensuing glow discharge was measured with an oscilloscope, all power supplies were deactivated after the arc discharge had stabilized. In Fig. 14 it should be noted that the glow discharge voltage was fixed by the geometry; thus, in order to increase the power added during the glow discharge period, it was necessary to change the ignitor supply loadline. In Fig. 16, the shape of the curve is thought to

depend on the thermal time constant of the cathode, i.e., how quickly the cathode can lose heat through radiation and conduction.

With the pulse flow method of starting, the cathode could ignite in milliseconds; however, different runs of the same cathode and between similar cathodes varied markedly. Figure 17 illustrates oscilloscope observations for configuration 4(a) (Fig. 5). On some runs, the cathode would break down, enter a single glow discharge mode lasting several milliseconds, and transition to a stable arc (Fig. 17(a)); however, during other runs of the same cathode at the same operating condition, the single glow discharge mode could last several seconds. Furthermore, during runs of the same cathode configuration (but a different cathode), the cathode was seen to jump from the glow discharge mode to the arc mode many times over the course of several seconds before a stable arc discharge was established (Fig. 17(b)). The reasons for these differences are unclear.

Arcing to cathode potential surfaces during the glow discharge period was observed. This phenomenon, first seen during the heaterless cathode tests in the J series thruster (discussed earlier), occurred during a glow discharge period when the combination of high gas pressures (>0.001 MMHG) and a plasma within the test facility (thruster chamber or bell jar) allowed the keeper and anode supplies (with open circuit voltages of approximately 100 V) to pass current. Arcing had not been observed during a pulse flow start in which the cathode ignited quickly (<1 sec) because the dual conditions of plasma and high gas pressure were not simultaneously present. This observation illustrates the importance of swift breakdown to arc transitions.

Dominant electron emission from the cathode orifice plate/cathode body at high total emission currents was once again observed despite the addition of the insert covering and the use of a diode for insert isolation (Fig. 11). However, in this configuration the current emitted by the insert cover/insert cover orifice plate could not be distinguished from the current emitted by the insert itself. Although in the diode connection, the cathode remains 1 to 2 V negative of the insert during arc operation, no performance differences were noted between diode operation and knife switch operation.

#### Accelerated Cyclic Ignition Test

To better understand the erosive mechanisms of heaterless ignition, an accelerated cyclic lifetest on configuration 4(b) (Fig. 18). Table 1 lists the operating conditions of the test. The cathode compiled 3430 successful starts out of 3550 ignition attempts (a successful start occurs when an arc discharge ignites during a cycle). Each cycle began by activating the keeper and ignitor power supplies, while opening the gas supply solenoid valve to release the gas pulse. (The anode supply was not used in this test.) Even though the power supplies and the solenoid valve were activated simultaneously, the power supplies reached their full open circuit voltages before the gas pulse released from the solenoid valve reached the cathode insert region. Once the gas reached the cathode insert region, the gas broke down electrically and a glow discharge ensued.

The glow discharge period usually ended with the transfer to an arc or, if the start is unsuccessful, after 15 sec with the shutdown of the ignitor supply. The keeper supply turned off 3 min later, quenching the arc (assuming a successful start) and the solenoid valve closed soon afterward. The cycle repeated itself 15 min after the beginning of the previous cycle. It is thought that the 11 min dormant interval in each cycle adequately simulates the ignition of a cold cathode (Fig. 16 and Table 1).

Figure 17(b) illustrates the oscilloscope observations of this cathode during the test. No significant variation in the traces were seen throughout the test; the elapsed time between voltage breakdown and a stable arc discharge remained at approximately 5 to 10 sec (as judged by observing the keeper voltmeter and current meter). Table 1 lists the heaterless cathode's electrical parameters for various cycles throughout the test. The keeper current and flowrate were not monitored and controlled closely; nevertheless, two trends can be observed. First, the keeper voltage increased incrementally throughout the test. Secondly, the insert emission current to total emission current (JI/JK) ratio remained constant at a given total emission current and maintained a value of nearly unity, in agreement with our previous observations at this total emission current level.

About half of the failed starts occurred because they occurred when the open circuit voltage of the keeper supply dropped to half of the initial value (this idiosyncrasy was due to the particular construction of our keeper supply.) These failed starts confirmed our observation that increased keeper supply voltage shortens the time spent in the glow discharge mode (see results of initial test). Because the ignitor supply would turn off before the cathode could transfer to the arc mode at the decreased keeper supply voltage, it is inferred that the glow discharge mode lasted longer at this lower value of keeper voltage. The other failed starts could not be explained.

The exterior cathode orifice plate appeared to suffer some sputter erosion as it appeared pockmarked and shiny; however the cathode orifice diameter did not change from its original 0.71 mm dimension (not shown). The exterior of the insert cover and the cover orifice plate also displayed the same scrubbed appearance noted on the cathode while the insert cover orifice did not change from its original 1.78 mm diameter (Fig. 19). The insert cover was cracked at the insert cover-orifice plate weld. This cracking occurred during testing and was probably exacerbated by flaring of one end of the cathode body (done with this test hardware to obtain a good electron beam weld of the tantalum insert cover to the 2 percent thoriated tungsten orifice plate).

In spite of the insert covering, the insert sustained damage. Normally the insert should slip out of the insert covering because the insert outside diameter is slightly smaller than the covering inside diameter; however, after the cycling test, the insert had fused to the insert covering and to the orifice plate (Fig. 19). Further, the insert displayed dimpling in a regular pattern. It is supposed that the insert did not make good electrical contact with the insert cover (which is necessary for the emission of copious numbers

from the insert during normal hollow cathode arc discharge operation) even though the insert was connected by three 15 cm lengths of rhenium wire. As a result, the insert connected itself electrically to the covering by arc discharges. Perhaps similar behavior could be observed with standard hollow cathodes, but the author is unaware of any other analogous observations.

### Summary and Conclusions

Heaterless ignition of inert gas ion thruster hollow cathodes was consistently achieved by using a high pressure region between the cathode and insert to reduce breakdown voltages at a given flowrate and to create conditions for the glow discharge/arc heating of the cathode. Limits to insert emission (for the insert isolated from the cathode) had been noted for total emission currents greater than 8 A. Linking the isolated insert to the cathode by use of a diode after arc ignition has been demonstrated. In response to concerns over insert erosion, a covering over the insert was added and the cathode was ignited with the use of a gas pulse. Millisecond ignition times were noted with gas pulse ignition, but differences in operation were observed for similar cathodes and test conditions. Operation of the covered insert caused anomalous fusing of the insert to the covering; however a suspected cause was postulated. Despite these difficulties, a 3550 cycle test with 3430 successful ignitions indicated that heaterless ignition of ion thruster hollow cathodes for thousands of cycles is feasible. Future work on heaterless hollow cathode ignition using the methods explored here should systematically determine what characteristics cause quick reliable ignition and what precisely are the life limiting effects through a full lifetest under the conditions envisioned for operation of these cathodes in a flight configuration.

### References

1. Rawlin, V.K., "Operation of J-Series Thruster Using Inert Gas," NASA TM-82977, 1982.
2. Sovey, J.S., "Improved Ion Containment Using A Ring-Cusp Ion Thruster," Journal of Spacecraft and Rockets, Vol. 21, No. 5, Sept.-Oct. 1984, pp. 488-495.
3. Hyman, J., "Hughes Research Laboratories Ion Propulsion Program," International Electric Propulsion Conference, 17th, Japan Society for Aeronautical and Space Science, Tokyo, 1984, pp. 160-167.
4. Rawlin, V.K., "Extended Operating Range of the 30-cm Diameter Ion Thruster With Simplified Power Processor Requirements," AIAA Paper 81-0692, Apr. 1981.
5. Mueller, L.A., "High Reliability Cathode Heaters for Ion Thrusters," AIAA Paper 76-1071, Nov. 1976.
6. Siegfried, D.E., "A Phenomenological Model for Orifed Hollow Cathodes," Ph.D. Thesis, Colorado State University, Dec. 1982. (also published as NASA CR-168026).

7. Siegfried, D.E. and Wilbur, P.J., "Advanced Ion Thruster Research," Colorado State University, Fort Collins, CO, Jan. 1984. (NASA CR-168340).
8. Beattie, J.R. and Matossian, J.N., "Mercury Ion Thruster Technology," NASA CN NAS3-23775, Nov. 1984.
9. Dulgeroff, C.R., Beattie, J.R., Poeschel, R.L., and Hyman, J., "IAPS (8-cm) Ion Thruster Cyclic Endurance Test," International Electric Propulsion Conference, 17th, Japan Society for Aeronautical and Space Science, Tokyo, 1984, pp. 250-260.
10. Cobine, J.D., Gaseous Conductors, Dover Publications, New York, 1958.
11. Von Engle, A., Ionized Gases, Clarendon Press, Oxford, 1955.
12. Druyvesteyn, M.J. and Penning, F.M., "The Mechanism of Electrical Discharges in Gases of Low Pressure," Reviews of Modern Physics, Vol. 12, No. 2, Apr. 1940, pp. 87-174.
13. Mirtich, M.J. and Kerlake, W.R., "Long Lifetime Hollow Cathodes for 30-cm Mercury Ion Thrusters," AIAA Paper 76-985, Nov. 1976.
14. Aston, G., "Ferm Cathode Operation in the Test Bed Ion Engine," International Electric Propulsion Conference, 17th, Japan Society for Aeronautical and Space Science, Tokyo, 1984, pp. 647-651.
15. Beattie, J.R., Private communication.
16. Williamson, W.S., "Characterization of 8-cm Engineering Model Thruster," Hughes Research Labs, Malibu, CA, Mar. 1984. (NASA CR-174673).

TABLE 1. - ACCELERATED CYCLIC LIFETEST CONDITIONS

[ $V_{KOC} = 110$  V;  $J_K = J_{KL}$ ;  $V_{IGOC} = 700$  V;  $J_{IGSC} = 1$  A; pulse volume ~30 sec; bell jar pressure: without flow -  $4 \times 10^{-7}$  torr; with flow -  $10^{-4}$  to  $10^{-5}$  torr. Cycle times: 0:00 - flow, ignitor supply, keeper supply on; 0:15 - ignitor supply off; 3:15 keeper supply off; 3:45 - flow off; 15:00 - repeat cycle.]

Cycle number	VK keeper voltage, V	JK keeper current, A	$\dot{m}$ mass flowrate (SCCM-xenon)	$J_i$ insert current, A
1	16	3.6	7.0	3.3
480	16.5	↓	6.3	↓
900	17.5	↓	↓	↓
1500	17.0	↓	↓	↓
<sup>a</sup> 1950	19.5	↓	↓	↓
2480	19.5	3.75	4.4	3.5
3020	20.5	3.75	7.2	3.5
3450	21.0	3.75	5.8	3.5

<sup>a</sup>Shutdown to replace empty xenon bottle.



ORIGINAL PAGE IS  
OF POOR QUALITY

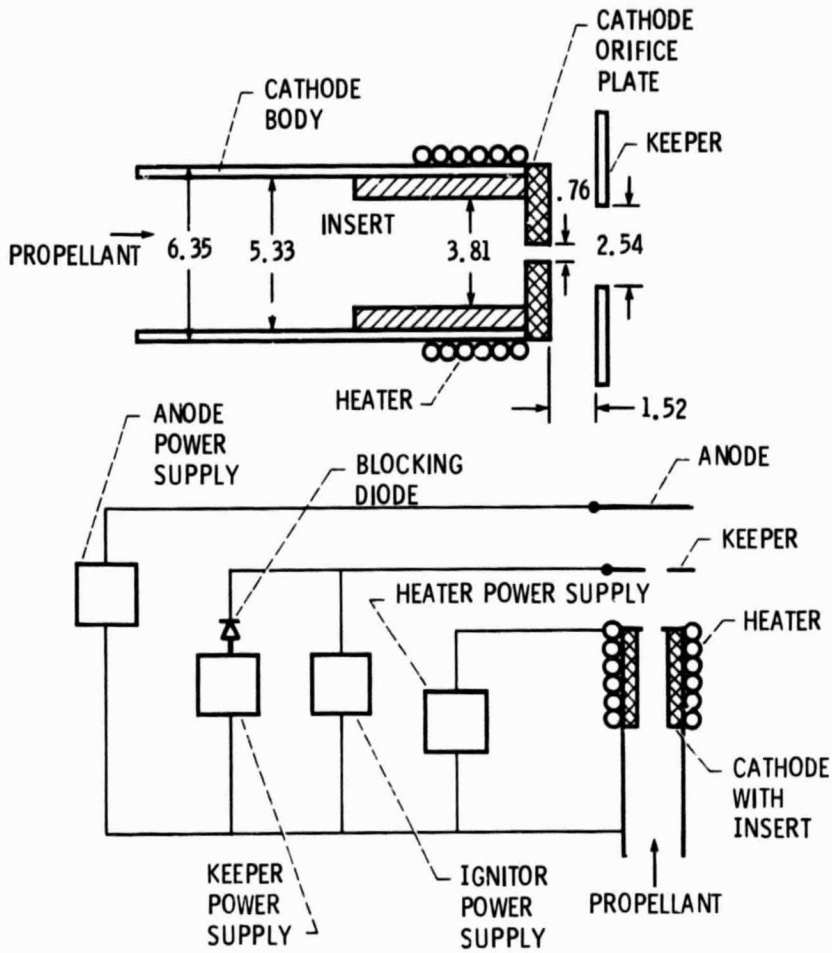
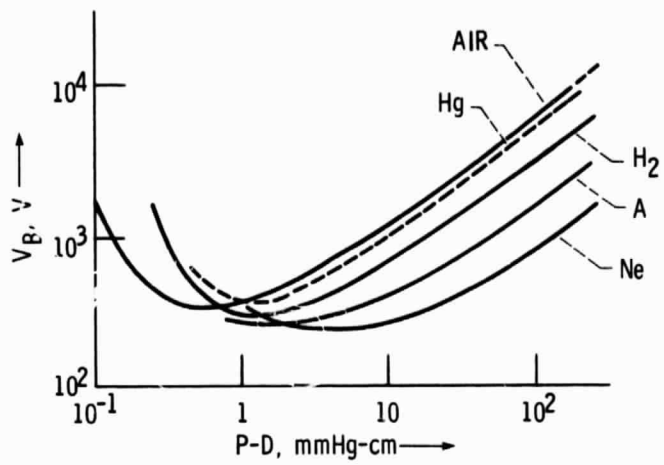


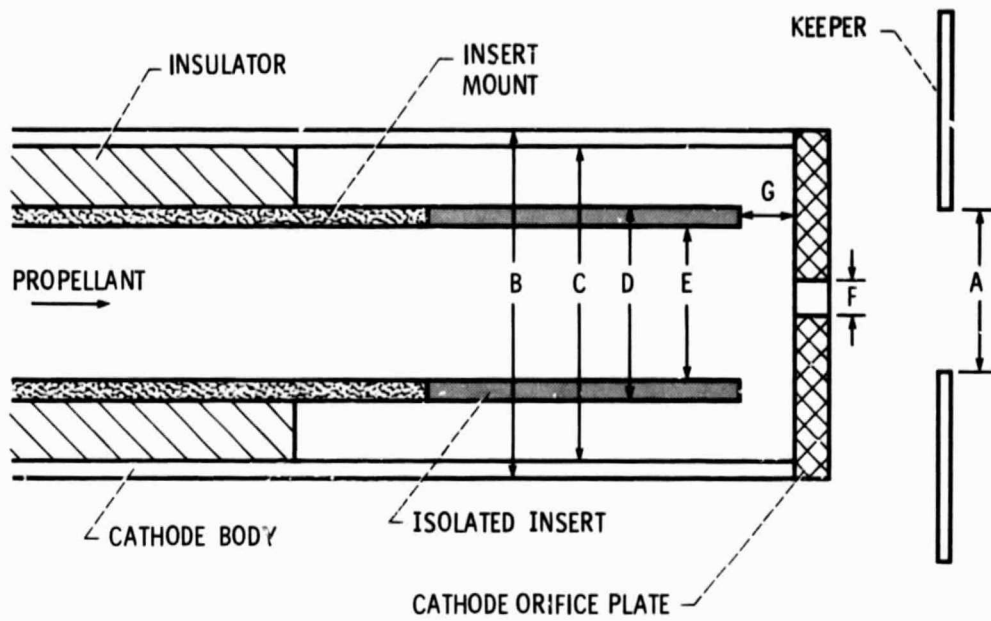
Figure 1. - Standard Ion thruster hollow cathode with open keeper. (30 cm ion thruster main cathode) (dimensions in mm)



MINIMUM BREAKDOWN VOLTAGE

GAS	CATHODE	VOLTS $V_{MIN}$	mm Hg cm (PD) $_{MIN}$
He	Fe	150	2.5
Ne	Fe	244	3.0
A	Fe	265	1.5
N <sub>2</sub>	Fe	275	0.75
O <sub>2</sub>	Fe	450	0.7
AIR	Fe	330	0.57
H <sub>2</sub>	Pt	295	1.25
CO <sub>2</sub>	?	420	0.5
Hg	W	425	1.8
Hg	Fe	520	~2
Hg	Hg	330	?
Na	Fe?	335	0.04

Figure 2. - Paschen's law (ref. 11).



DIMENSIONS, mm

A	B	C	D	E	F	G	CONFIGURATION IDENTIFIER
2.54	6.35	5.59	2.29	1.19	.38	.76	1a
					.76	.38	1b
						.76	1c
						3.05	1d
						6.35	1e
					1.27	.76	1f
2.54	9.53	7.37	5.33	3.81	.76	.76	2a
					1.27	5.33	2b
2.54	12.7	11.68	5.33	3.81	.43	.76	3a
					.76	.76	3b

Figure 3. - Original heaterless hollow cathode.

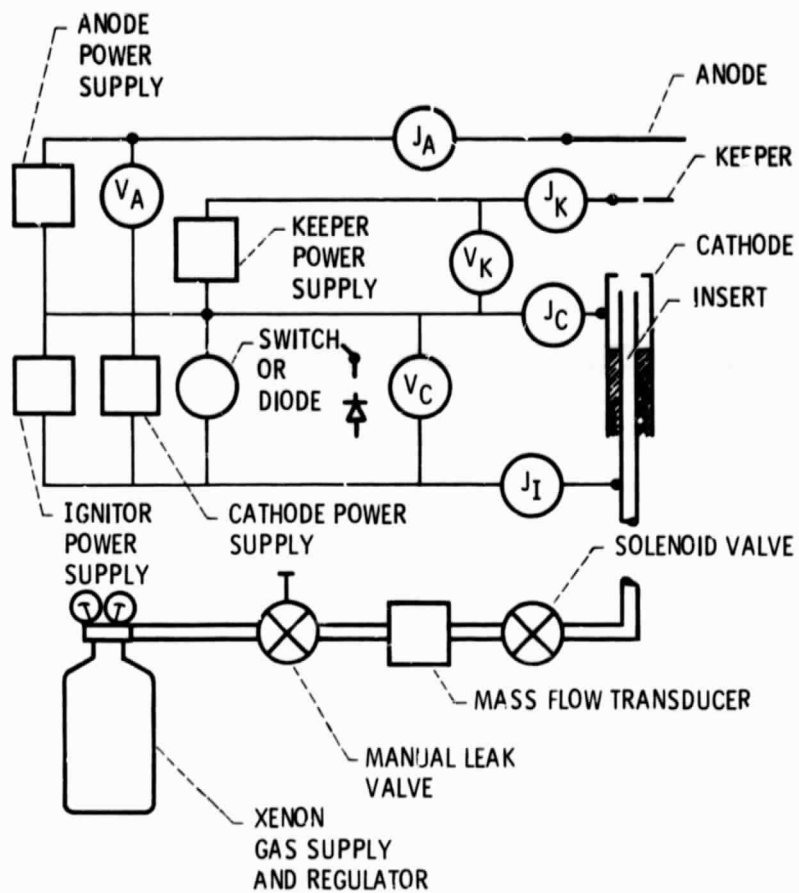
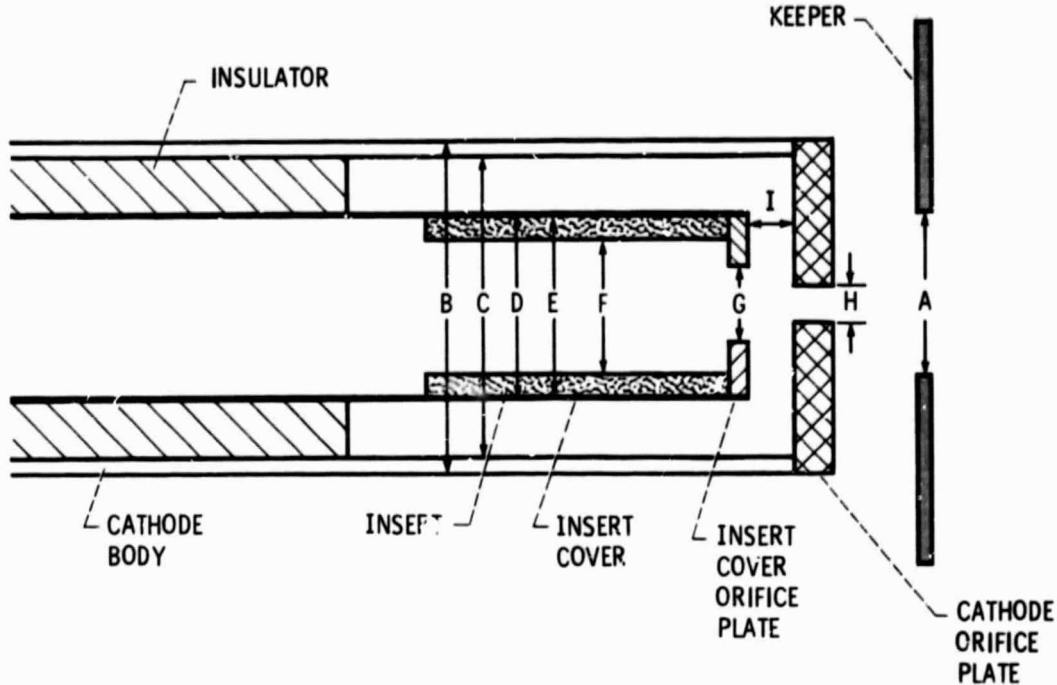


Figure 4. - Heaterless cathode power supply and flow arrangement.

ORIGINAL PAGE IS  
OF POOR QUALITY



DIMENSIONS, mm

A	B	C	D	E	F	G	H	I	CONFIGURATION IDENTIFIER
2.54	12.7	11.68	6.35	5.46	3.81	1.27	.76	.76	4a
						1.78	.76	.76	4b

Figure 5. - Modified heaterless hollow cathode.

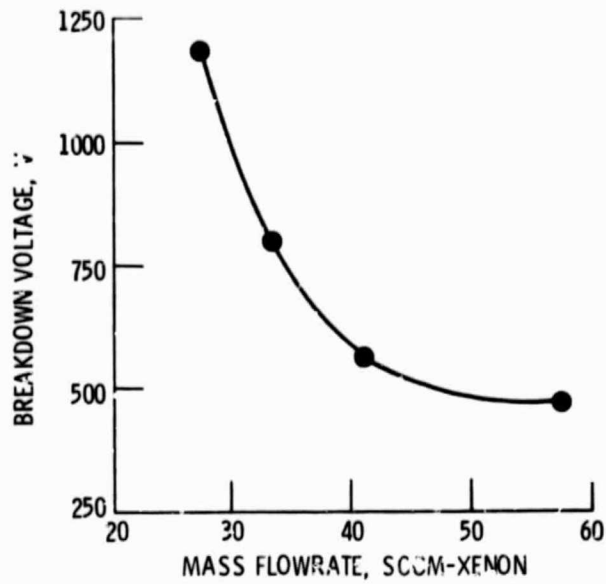


Figure 6. - Breakdown voltage vs flowrate for standard hollow cathode.

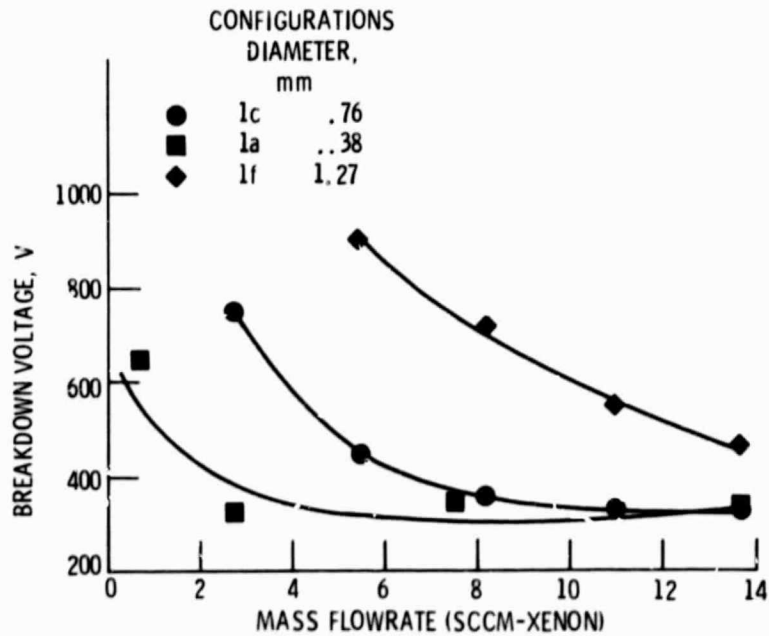


Figure 7. - Breakdown voltage to flowrate effect of cathode orifice diameter (dimension F, Figure 3).

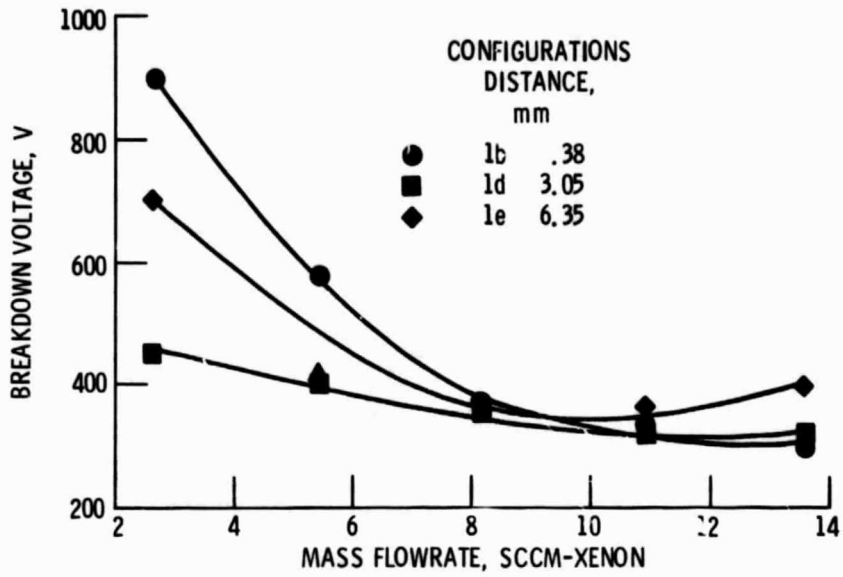


Figure 8. - Breakdown voltage vs flowrate effect of insert cathode distance (dimension 6, Fig. 3).

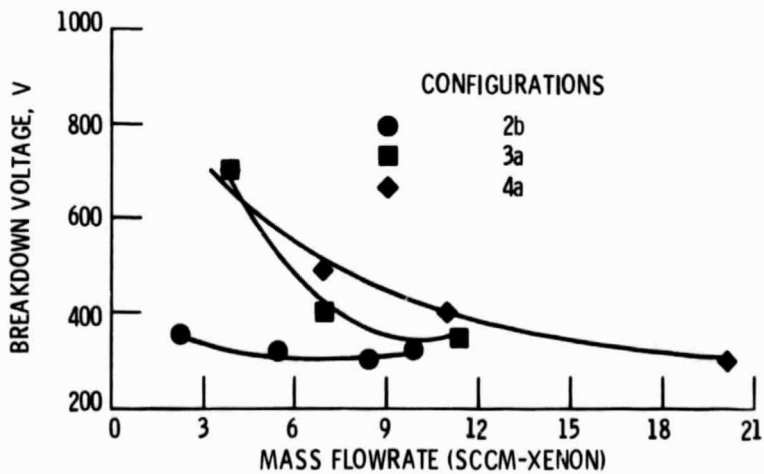


Figure 9. - Breakdown voltage vs flowrate original and modified heaterless geometrics (Figures 3 and 5).

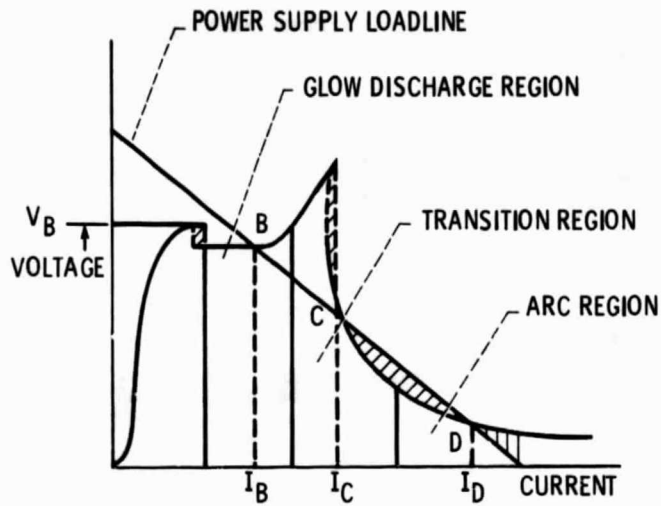


Figure 10. - V-I characteristic for gaseous discharge (ref. 10).

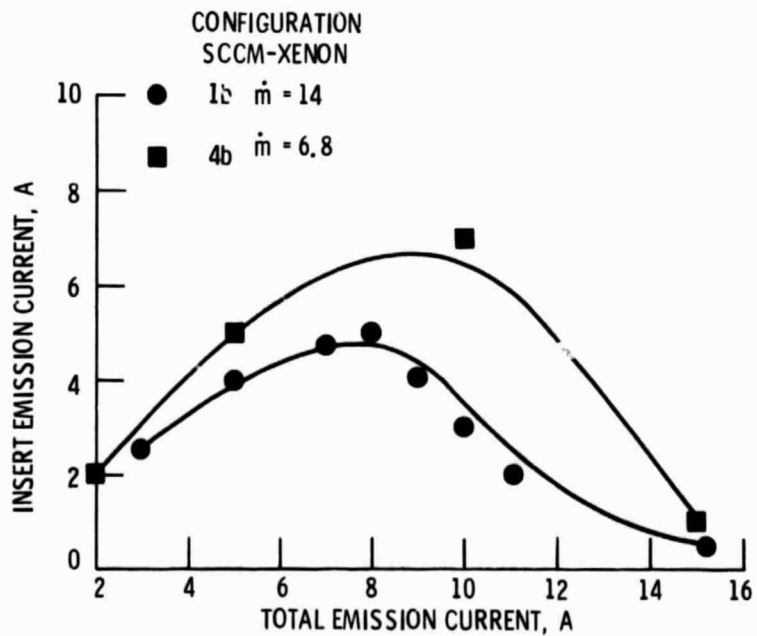
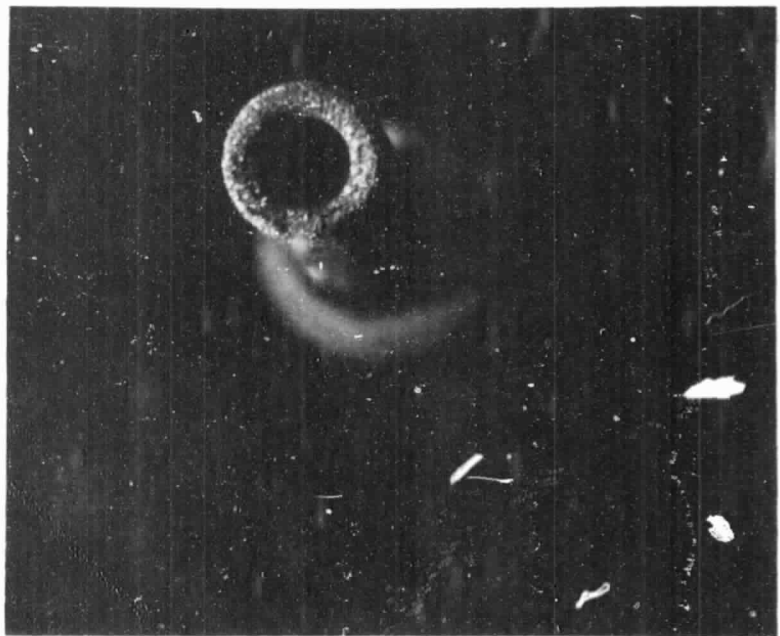
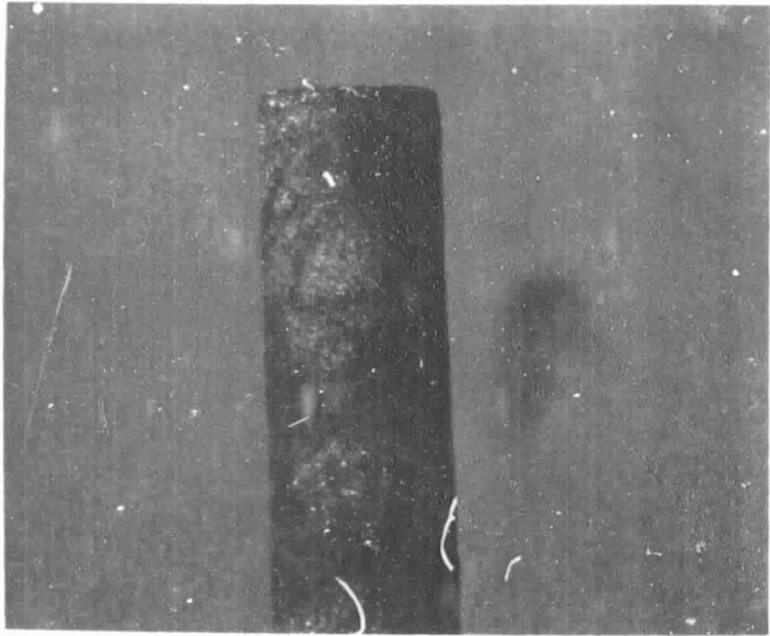


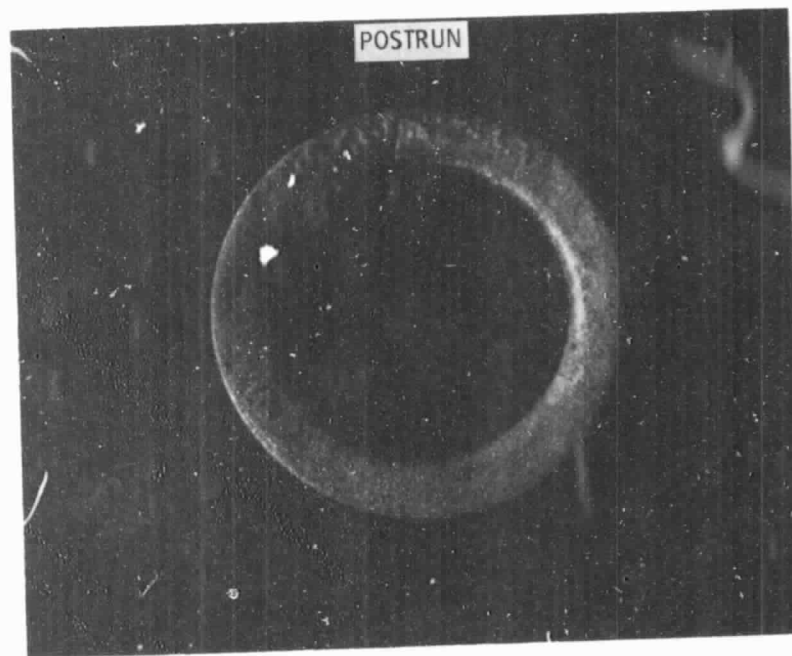
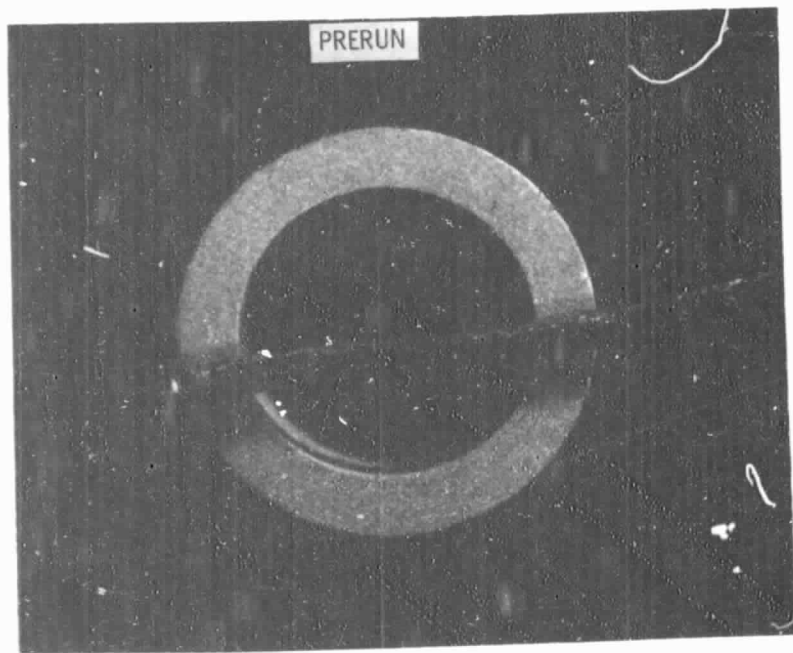
Figure 11. - Insert emission current vs total emission current.





ORIGINAL PAGE IS  
OF POOR QUALITY

Figure 12. - Postrun photos of insert in original heaterless hollow cathode tests (Configuration 1c).



0.51mm wire in above picture for scaling.

Figure 13. - Prerun and postrun photos of insert in original heaterless hollow cathode tests (Configuration 3b).

ORIGINAL PAGE IS  
OF POOR QUALITY

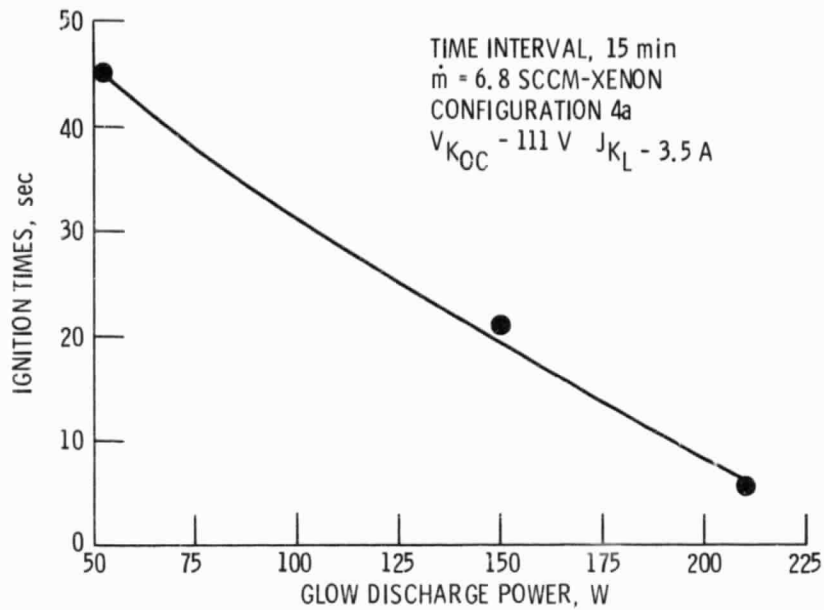


Figure 14. - Glow discharge lifetime vs glow discharge power. (configuration 4a)

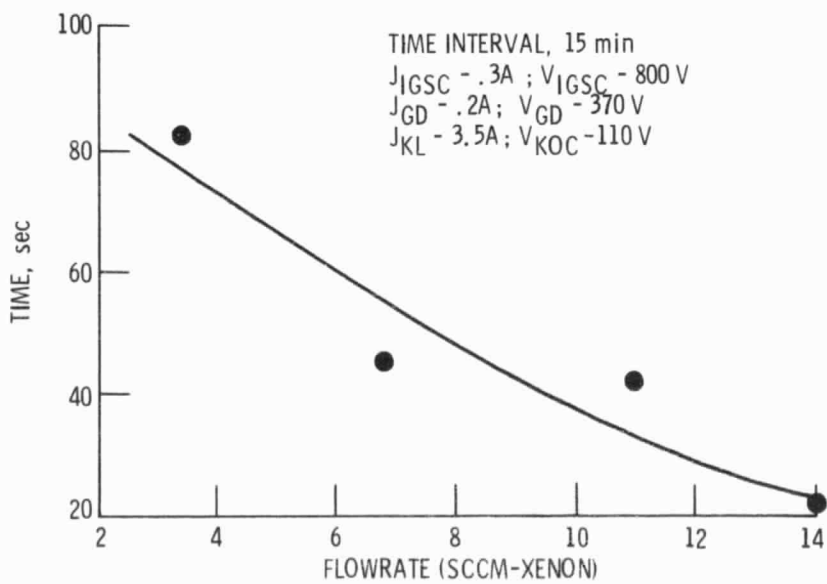


Figure 15. - Glow discharge lifetime vs flowrate. (configuration 4a)

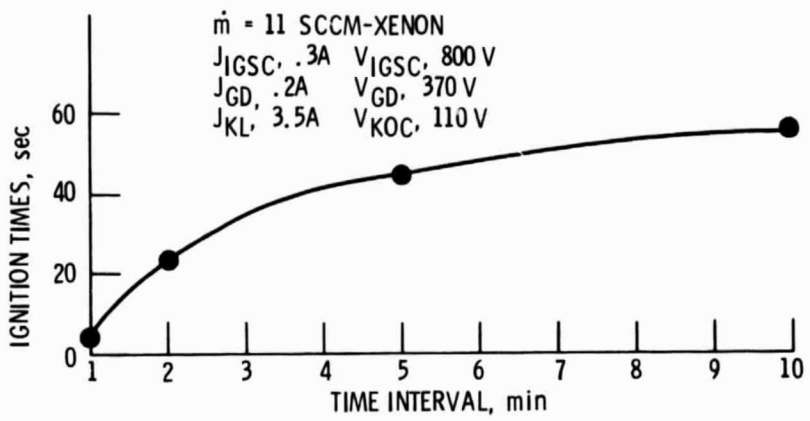


Figure 16. - Glow discharge lifetime vs time interval. (configuration 4a)

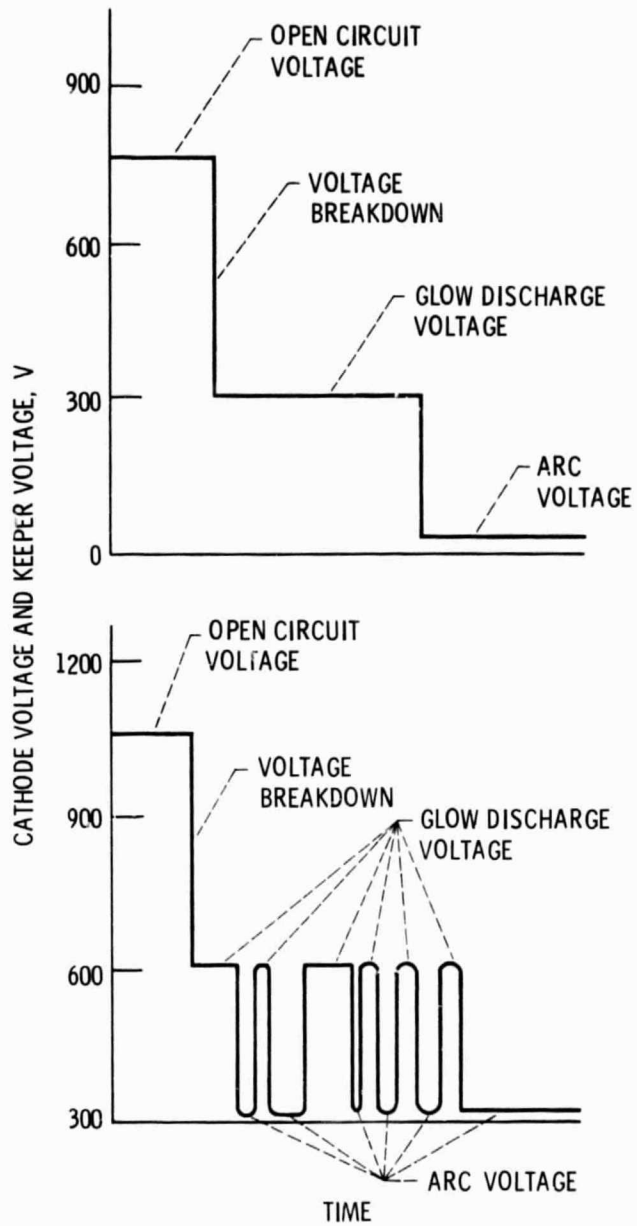
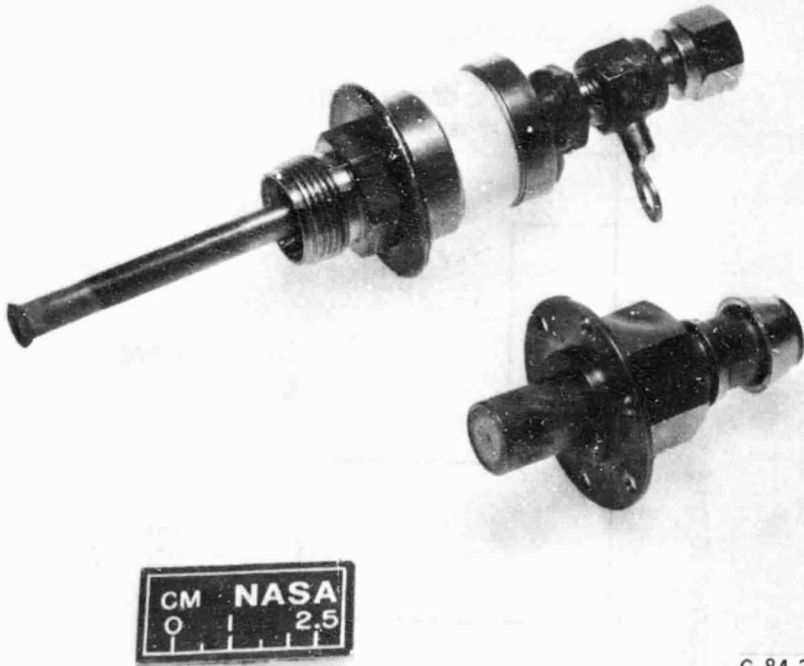


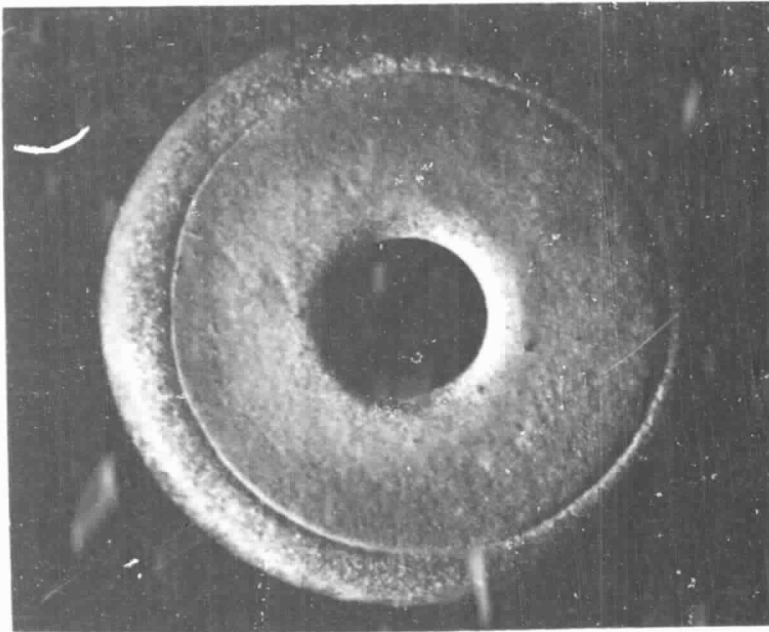
Figure 17. - Voltage vs time - pulsed flow ignition.

ORIGINAL PAGE IS  
OF POOR QUALITY

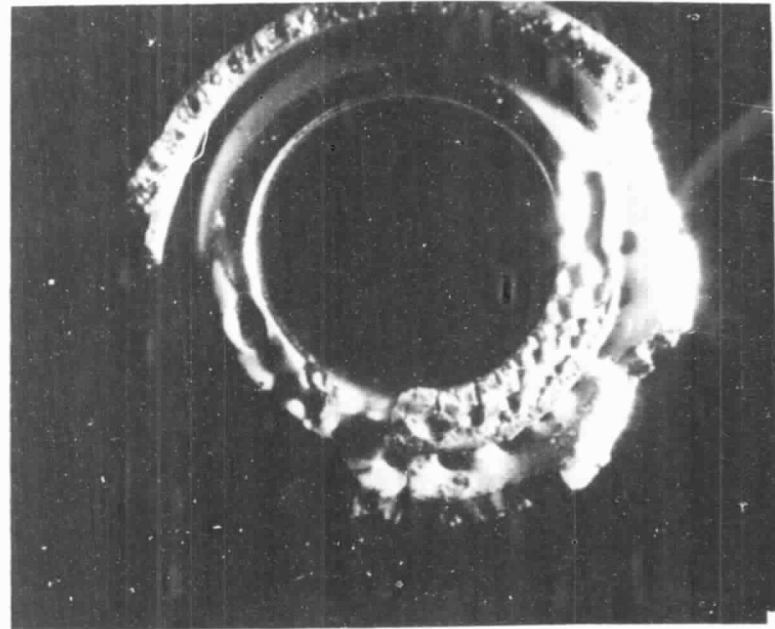


C-84-3940

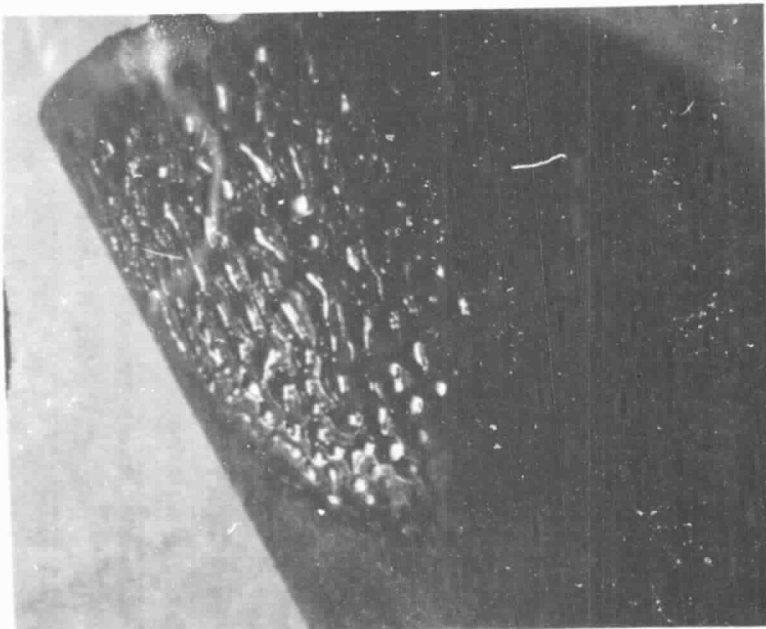
Figure 18. - Modified heaterless hollow cathode.



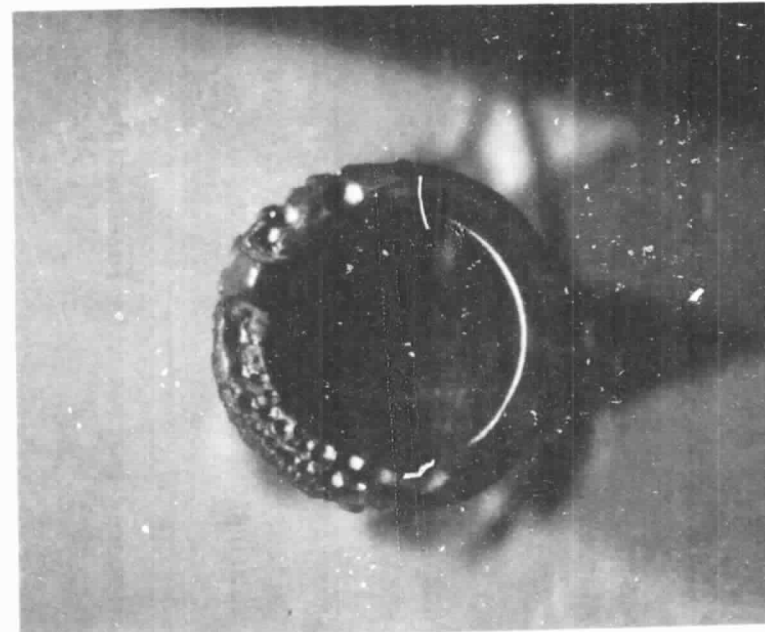
(a) Insert cover orifice plate (looking upstream)



(b) Same view as (a) after removing orifice plate.



(c) Insert after removing cover.



(d) Insert after removing cover.

Figure 19. - Photos of accelerated cyclic lifetest hardware after 3550 cycles.

ORIGINAL PAGE IS  
OF POOR QUALITY

1. Report No. NASA TM-87086		2. Government Accession No.		3. Recipient's Catalog No.	
4. Title and Subtitle Heaterless Ignition of Inert Gas Ion Thruster Hollow Cathodes				5. Report Date	
				6. Performing Organization Code 506-55-22	
7. Author(s) Michael F. Schatz				8. Performing Organization Report No. E-2672	
				10. Work Unit No.	
9. Performing Organization Name and Address National Aeronautics and Space Administration Lewis Research Center Cleveland, Ohio 44135				11. Contract or Grant No.	
				13. Type of Report and Period Covered Technical Memorandum	
12. Sponsoring Agency Name and Address National Aeronautics and Space Administration Washington, D.C. 20546				14. Sponsoring Agency Code	
15. Supplementary Notes Prepared for the 18th International Electric Propulsion Conference, cosponsored by the AIAA, JSASS, and DGLR, Alexandria, Virginia, September 30-October 2, 1985.					
16. Abstract Heaterless inert gas ion thruster hollow cathodes were investigated with the aim of reducing ion thruster complexity and increasing ion thruster reliability. In this study, cathodes heated by glow discharges were evaluated for power requirements, flowrate requirements, and life limiting mechanisms. In addition, an accelerated cyclic life test was completed.					
17. Key Words (Suggested by Author(s)) Inert gas; Cathode; Hollow cathode; Ion thrusters			18. Distribution Statement Unclassified - unlimited STAR Category 20		
19. Security Classif. (of this report) Unclassified		20. Security Classif. (of this page) Unclassified		21. No. of pages	22. Price*